Broad spectrum measurement of the birefringence of an isothiocyanate based liquid crystal

Oksana Trushkevych[1],* Huan Xu[1] Tianxin Lu[1] J. Axel Zeitler[2] Rakchanok Rungsawang[3] Felix Gölden[4] Neil Collings[1] and William A. Crossland[1]
[1]Centre for Advanced Photonics and Electronics, Engineering Department, Cambridge, CB3 0FA, UK
[2]Department of Chemical Engineering and Biotechnology, Cambridge, CB2 3RA, UK
[3]Semiconductor Physics Group, Cavendish Laboratory, Cambridge, CB3 0HE, UK
[4]Microwave Engineering, Technische Universität Darmstadt, 64283, Germany
*Corresponding author. ot213@cam.ac.uk

Tunable materials with high anisotropy of refractive index and low loss are of particular interest in the microwave and terahertz range. Nematic liquid crystals are highly sensitive to electric and magnetic fields and may be designed to have particularly high birefringence. In this paper we investigate birefringence and absorption losses in an isothiocyanate based liquid crystal (designed for high anisotropy) in a broad range of the electromagnetic spectrum, namely 0.1–4 GHz, 30 GHz, 0.5–1.8 THz, and in the visible and near-infrared region (400 nm–1600 nm). We report high birefringence (Δn = 0.19 − 0.395) and low loss in this material. This is attractive for tunable microwave and terahertz device applications.

1. Introduction

Liquid crystals (LCs) have long been known as highly anisotropic materials in the visible range. Their anisotropy and sensitivity to external fields have led to numerous display and nondisplay applications. Moreover, LCs are very promising materials at microwave [1–8] and terahertz (THz) frequencies [9–13] due to low losses and comparatively high anisotropy. LCs are particularly suitable for operation at frequencies beyond 10 GHz as the dielectric loss decreases with increasing frequency [14], making them attractive for phase modulating devices. Due to the display mass market LC materials are accessible, and fabrication methods can be derived from display technology that can make LC based microwave devices highly cost effective [15]. Some LC compounds have been shown to possess a large anisotropy at microwave frequencies [8,16]. The dielectric anisotropy in the microwave region correlates with the material's birefringence in the visible range [8]. One class of materials with particularly high optical birefringence is isothiocyanates [17]. The molecular weight of such compounds is 250–400 a.u. Here a commercially available LC material specially designed for high birefringence in the visible range ($\Delta n_{\lambda=589\ nm} = 0.38$) was studied in other parts of the electromagnetic spectrum, i.e., the GHz, THz, and IR regions.

2. Sample Preparation and Experimental Methods

The liquid crystal LCMS-107 was purchased from LCMS Ltd. Co. The compound is a mixture of isothiocyanates (rod-shaped molecules) and possesses a nematic phase with positive dielectric anisotropy in a wide temperature range between Tm < −20 °C and Tc = 110 °C. Its ordinary and extraordinary refractive indices as specified by the manufacturer at λ = 633 nm are $n_o = 1.535$ and ne = 1.915, and the resulting anisotropy of the refractive index is unusually high, Δn = 0.38.

The spectroscopic studies were conducted at room temperature (21–23 °C), within the nematic phase of the material. In bulk form nematic LCs arrange as randomly oriented domains of ordered molecules. The size of such domains is of the order of the optical wavelength, leading to strong light scattering. Therefore, in bulk, LCs appear milky. To access the anisotropic properties of LCs they must be aligned either by an external electric or magnetic field, or in thin layers (up to 200 µm) by a special treatment of the holding cell surfaces. When aligned, nematic LCs have a preferential direction in which the rod-shaped molecules are oriented, which is called the director. Along the director the extraordinary refractive index is observed. Ordinary refraction is in the plane perpendicular to the director. In this paper we will refer to the refractive indices with respect to the nematic director (and molecular alignment) as perpendicular $n\perp = no$ and parallel $n\parallel = ne$.

In the 0.1–4 GHz study, the LC sample was sandwiched between a pair of gold plated brass electrodes to form a capacitor at the end of a transmission line. The complex dielectric permittivity was calculated by measuring the complex reflection coefficient of both the filled and the unfilled capacitor [8]. The LC film thickness was defined by spacers set outside the active area. First, an empty cell was measured and its thickness was calculated based on the dielectric permittivity of the air. The calculated thickness was 30 µm +/-1 µm. Then LC was introduced into the cell by capillary action. The LC films were planar-aligned by coating the electrodes with a polyimide alignment agent and rubbing. An electric field up to 40 V AC (1 kHz) was applied to the sample to switch it into a homeotropic geometry. In this way, the parallel ($\varepsilon\parallel$) and the perpendicular ($\varepsilon\perp$) components of the dielectric permittivity were measured.

For the 30 GHz measurement, we used the resonant cavity perturbation method [18]. The LC material in a polytetrafluoroethylene (PTFE) capillary with an inside diameter of 360 µm is introduced into a cavity and perturbs the resonant field. This perturbation results in a small shift of the frequency and the full width at half-maximum (FWHM) of the resonance. By evaluating this shift, the dielectric properties $\varepsilon 0$ and ε'' can be extracted. The LC inside the PTFE capillary is oriented parallel ($\varepsilon\parallel$) or perpendicular ($\varepsilon\perp$) to the electric field in the resonator by a magnetic field of 0.5 T. The resonator has an unloaded quality factor of 3300. which allows extracting loss tangents down to 5×10^{-3}.

Terahertz time-domain spectroscopy [19] was performed with a setup similar to that described previously [20,21]. The measurements were conducted in the nitrogen atmosphere (humidity ~4%) to reduce THz absorption by water vapour molecules. Two quartz plates were coated with an alignment agent (polyimide) and rubbed to achieve planar alignment. The LC was filled into a 130 µm gap between the plates by the capillary force. Temporal waveforms were acquired through the quartz plates in direct contact with one another and the filled cell to remove absorption of the quartz. If the gap is retained, the empty cell acts as an interferometer and gives multiple reflections. Once the LC is inserted into the gap, the refractive indices are better matched and the reflections are dramatically reduced. The measurement on the quartz plates was used as the reference waveform in the subsequent analysis. The complex refractive index was extracted from the terahertz time-domain waveform, which contains both amplitude and phase information. Fast Fourier transform (FFT) was performed to extract the magnitude and the phase of the signal as a function of frequency. In our experiments the terahertz pulse propagated from free space through the first quartz window of the sample cell, the LC sample, the second quartz window, and back to free space. Prior to FFT the time-domain waveform was cut after 26 ps to avoid etalon reflections of the sample pulse being reflected from the quartz window

interfaces. The transmitted waveform represents the summation of an infinite series of decaying echo reflections from the LC sample between the two quartz windows. The optical constants were extracted in a similar approach to that described by Pupeza, Wilk, and Koch [22]. The terahertz waves were linearly polarized, and the values for the parallel and the perpendicular complex refractive index were obtained by rotating the planar aligned cell around the terahertz propagation axis in order to probe both components.
Near IR–visible absorption spectroscopy (400 nm to 1600 nm) was performed on a similar quartz cell with a 130 µm thickness and planar polyimide alignment layers. The probe beam was linearly polarized, and the measurement was repeated for both vertical and horizontal orientations of the planar cell. The method of performing birefringence studies in the near IR and the visible part of the spectrum was described earlier [23]. The LC was filled by capillary action into glass cells with 10 µm and 5 µm gaps. The cells had transparent indium tin oxide (ITO) electrodes and planar polyimide alignment layers. A cell is placed between a polarizer and an analyzer so that a light wave propagates through the cell with its polarization axis at an angle of 45° to LC alignment direction. It introduces a phase retardation $\delta = 2\pi d\Delta n/\lambda$, where λ is the wavelength of light and d is the thickness of the LC sample. The transmitted intensities $I_{\perp}$ and $I_{\parallel}$, corresponding, respectively, to the perpendicular and parallel orientations of the analyzer relative to the polarizer are measured.
The phase difference introduced by the LC layer is given by [23].

$$||\delta| = N\pi + 2tan^{-1}\sqrt{\frac{I_{\perp}}{I_{||}}}, \quad N = 0,2,\ldots \tag{1}$$

$$|\delta| = (N+1)\pi + 2tan^{-1}\sqrt{\frac{I_{\perp}}{I_{||}}}, \quad N = 1,3,\ldots \tag{2}$$

N is determined by switching with external electric field into homeotropic geometry (and thus reducing anisotropy to zero). The birefringence of the LC is obtained from δ through the relations (1) and (2).

3. Experimental Results

The spectroscopic measurements of the refractive indices for the spectral regions 0.1–4 GHz, 30 GHz, and 0.5–1.8 THz are presented in Figs. 1 and 2. The values of the refractive index in the terahertz region and at 30 GHz both perpendicular and parallel to the alignment direction were lower compared to the values in the optical range (Table 1), which is expected and is in agreement with previous research on other nematic LCs in the terahertz [1,13,24] and gigahertz [3,25] regions. Importantly, in both GHz and THz regions of the spectrum the birefringence in LCMS is much higher than of the LCs based on cyanobiphenyls. In particular, in the THz range the birefringence of LCMS107 was measured to be between 0.19 and 0.33 compared to commonly used nematics like cyanobiphenyl mixture E7 ($\Delta n = 0.152$) at 0.2–1.2 THz [26] and a family of cyanobiphenyls with Δn between 0.078 and 0.106 [13]. Around 0.1 GHz there is a relaxation in a perpendicular component of LCMS107 liquid crystal [8] that is visible as a decrease in the perpendicular refractive index [Fig. 1(a)]. There are no sharp features in the THz part of the spectrum (Fig. 2). The losses in the GHz range are usually expressed in the form of the imaginary part of the dielectric constant ε″, or the loss tangent $tan\ \delta = \varepsilon''/\varepsilon 0$. In the present material in the GHz range the

dielectric losses are low (Table 1). This is consistent with what has been reported in other LC materials [14]. The values at 30 GHz are very attractive for device applications.
The dielectric loss, ε", and the absorption coefficient, α, commonly used at optical frequencies are related as follows.

$$\alpha = (4\pi f n k)/c;\ k = \varepsilon''/2n \quad (3)$$

where f is the frequency of the wave and c is the speed of light, both in vacuum; n and k are the refractive index and the attenuation index of the media, respectively. Expressed this way, absorption has a linear dependence of frequency, and exhibits an increase with increasing frequency. The investigated LC had low absorption in the near infrared range and moderate absorption in a part of the visible spectrum (Fig. 3). We attribute the absorption at shorter wavelengths (<500 nm) to electronic transitions that are stronger along the longer axis of the rod-like molecules. In the near infrared, the absorption in LCs is influenced by the existence of molecular relaxations in the mid and far IR [27].
Interestingly, in the visible range the absorption for the parallel orientation is stronger, while at 0.1–4 GHz and 30 GHz the absorption is stronger for the perpendicular component (Figs. 1 and 2 and Table 1). This is in line with published reports in other nematic LCs [8,13]. For frequencies up to 1 THz, $\alpha\parallel > \alpha\perp$; however, the perpendicular component of absorption grows faster than the parallel component, and above 1 THz it becomes higher than the parallel component of absorption $\alpha\perp > \alpha\parallel$. Relaxations at higher frequencies may be responsible for the reversal of the relative magnitude of the parallel and perpendicular absorption coefficients observed in the IR and visible region. The birefringence (Table 1) remains high throughout the studied parts of the electromagnetic spectrum. It is therefore promising to use this material at frequencies around 30 GHz and 1–1.6 THz, where the losses are low and the birefringence is significant.

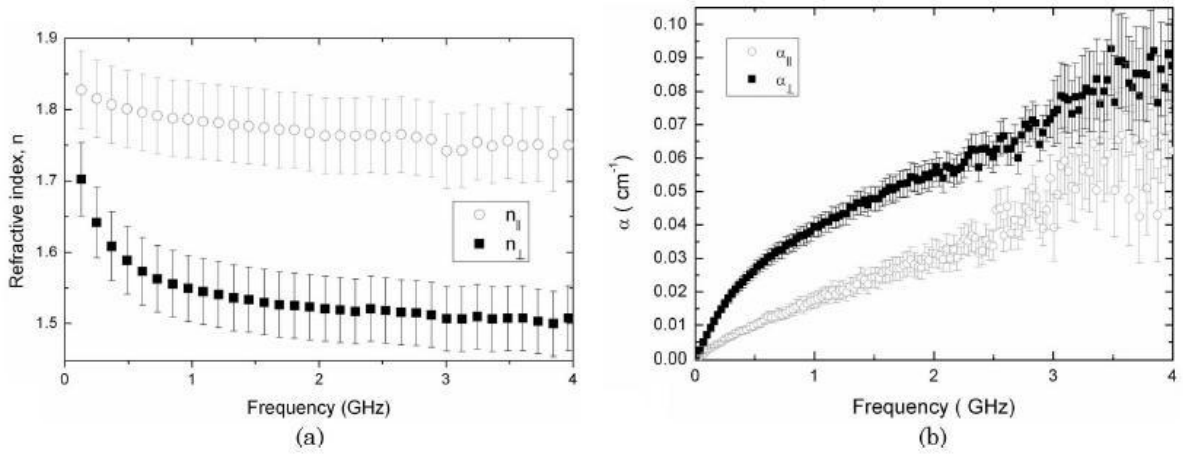

Fig. 1. Frequency-dependent ordinary and extraordinary (a) refractive indices and (b) absorption coefficients in liquid crystal LCMS-107 at 0.1–4 GHz.

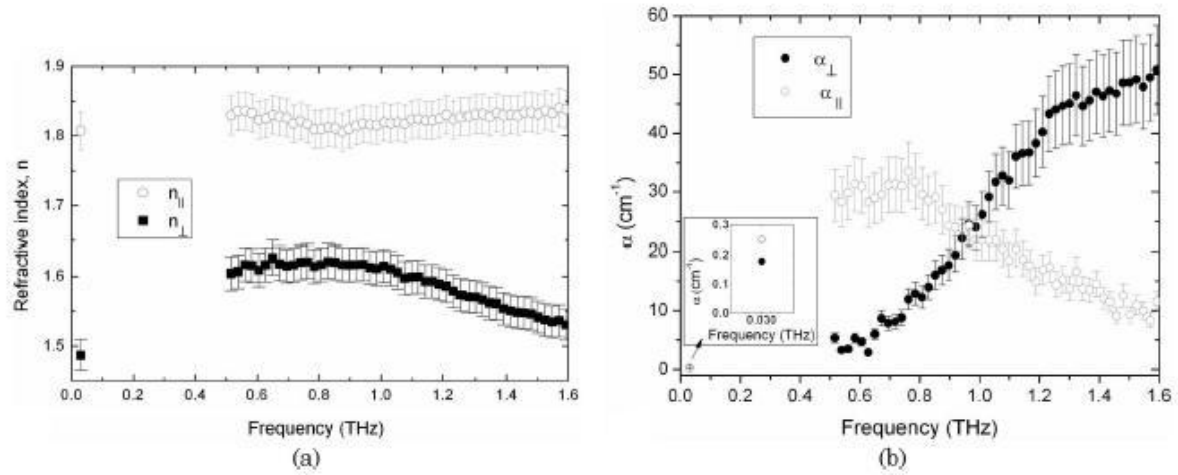

Fig. 2. Frequency-dependent ordinary and extraordinary (a) refractive indices and (b) absorption coefficients in liquid crystal LCMS-107 at 30 GHz and 0.5–1.8 THz (absorption at 30 GHz was measured as dielectric loss ε″ and converted to absorption coefficient).

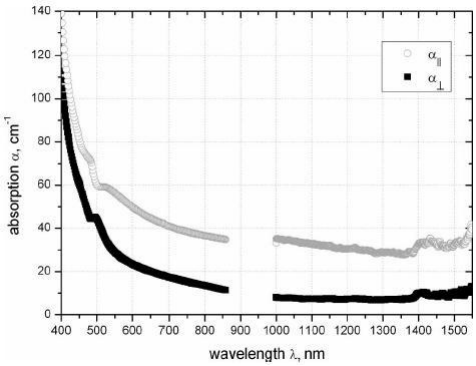

Fig. 3. Absorption in liquid crystal LCMS-107 in the near IR and visible.

Frequency/ Wavelength	$n_\perp$	$n_\parallel$	$\alpha_\perp$	$\alpha_\parallel$	Δn
$f = 3$ GHz	1.51 ± 0.02	1.76 ± 0.03	0.08 cm^{-1}	0.05 cm^{-1}	0.25 ± 0.05
$f = 30$ GHz	1.487 ± 0.005	1.882 ± 0.005	0.25 cm^{-1}	0.18 cm^{-1}	0.39 ± 0.01
$f = 1$ THz	1.62 ± 0.02	1.83 ± 0.03	23 cm^{-1}	23 cm^{-1}	0.21 ± 0.05
$f = 1.5$ THz	1.54 ± 0.02	1.83 ± 0.03	49 cm^{-1}	10 cm^{-1}	0.29 ± 0.05
$f = 1.8$ THz	1.51 ± 0.02	1.84 ± 0.03	35 cm^{-1}	2 cm^{-1}	0.33 ± 0.05
$\lambda = 1550$ nm	-	-	13 cm^{-1}	40 cm^{-1}	0.32 ± 0.01
$\lambda = 800$ nm	-	-	12 cm^{-1}	36 cm^{-1}	0.34 ± 0.01
$\lambda = 633$ nm	-	-	20 cm^{-1}	30 cm^{-1}	0.37 ± 0.01
$\lambda = 633$ nm	1.535 [a]	1.915 [a]	-	-	0.380 [a]

[a] As quoted by the manufacturer.

Table 1. Refractive Indices, Birefringence, and Absorption Values at Different Frequencies and Wavelengths in Liquid Crystal LCMS-107

4. Conclusions

A nematic liquid crystal with a large birefringence in the visible range ($\Delta n_{\lambda=633} = 0.38$) is shown to possess a high birefringence in the microwave ($\Delta n \sim 0.25$ at 0.1–4 GHz and $\Delta n = 0.395$ at 30 GHz) and terahertz frequencies ($\Delta n \sim 0.19 – 0.32$ at 0.5–1.8 THz) and in the infrared region ($\Delta n \sim 0.32 – 0.34$). Such high birefringence values are very promising for device applications, in particular around 30 GHz, and in those terahertz applications where the amount of absorption ($\alpha \sim 30$ cm^{-1}) can be tolerated, as, for example, in the case of thin films for phase modulating and beam forming devices.

The authors acknowledge funding from the Engineering and Physical Sciences Research Council (EPSRC) Platform Grant (GR/S12074/02) and the Centre for Advanced Photonics and Electronics (CAPE). Current CAPE partners are Dow Corning Ltd. and Alps Electric Co., Ltd. J. A. Zeitler would like to thank Gonville & Caius College for funding through a research fellowship.

References

1. T. Nose, S. Sato, K. Mizuno, J. Bae, and T. Nozokido, "Refractive index of nematic liquid crystals in the submillimeter wave region," Appl. Opt. 36, 6383–6387 (1997).
2. H. Fujikake, T. Kuki, H. Kamoda, F. Sato, and T. Nomoto, "Voltage- variable microwave delay line using ferroelectric liquid crystal with aligned submicron polymer fibers," Appl. Phys. Lett. 83, 1815–1817 (2003).
3. C. Weil, S. Muller, P. Scheele, P. Best, G. Lussem, and R. Jakoby, "Highly-anisotropic liquid-crystal mixtures for tunable microwave devices," Electron. Lett. 39, 1732–1734 (2003).
4. Y. Utsumi, T. Kamei, and R. Naito, "Measurements of effective dielectric permittivity of microstrip-line-type liquid crystal devices using inductive coupled ring resonator," Electron. Lett. 39, 849–851 (2003).
5. F. Yang and J. R. Sambles, "Microwave liquid-crystal variable phase grating," Appl. Phys. Lett. 85, 2041–2043 (2004).
6. T. Nose, M. Honma, T. Nozokido, and K. Mizuno, "Simple method for the determination of refractive indices and loss parameters for liquid-crystal materials in the millimetre wave region," Appl. Opt. 44, 1150–1155 (2005).
7. F. Goelden, A. Lapanik, A. Gaebler, S. Mueller, W. Haase, and R. Jakoby, "Systematic investigation of nematic liquid crystal mixtures at 30 GHz," in LEOS Summer Topical Meetings, 2007 Digest of the IEEE (IEEE, 2007), pp. 202–203.
8. H. Xu, O. Trushkevych, N. Collings, and W. A. Crossland, "Measurement of dielectric permittivity modulation of some liquid crystals for microwave applications," Mol. Cryst. Liq. Cryst. 502, 235–244 (2009).
9. C.-Y. Chen, C.-L. Pan, C.-F. Hsieh, Y.-F. Lin, and R.-P. Pan, "Liquid-crystal-based terahertz tunable Lyot filter," Appl. Phys. Lett. 88, 101107 (2006).
10. I.-C. Ho, C.-L. Pan, C.-F. Hsieh, and R.-P. Pan, "Liquid-crystal based terahertz tunable Solc filter," Opt. Lett. 33, 1401–1403 (2008).
11. C.-F. Hsieh, Y.-C. Lai, R.-P. Pan, and C.-L. Pan, "Polarizing terahertz waves with nematic liquid crystals," Opt. Lett. 33, 1174–1176 (2008).
12. T.-R. Tsai, C.-Y. Chen, R.-P. Pan, C.-L. Pan, and X.-C. Zhang, "Electrically controlled room temperature terahertz phase shifter with liquid crystal," IEEE Microw. Wireless Compon. Lett. 14, 77–79 (2004).
13. R. Wilk, N. Vieweg, O. Kopschinski, T. Hasek, and M. Koch, "THz spectroscopy of liquid crystals from the CB family," J. Infrared Millim. Waves 30, 1139–1147 (2009).
14. S. Mueller, F. Goelden, P. Scheele, M. Wittek, C. Hock, and R. Jakoby, "Passive phase shifter for W-band applications using liquid crystals," in Proceedings 36th European Microwave Conference (2006), pp.306–309.
15. F. Goelden, A. Gaebler, A. Manabe, M. Goebel, S. Mueller, and R. Jakoby, "Novel tunable liquid crystal phase shifter for microwave frequencies," Electron. Lett. (to be published).

16. S. Mueller, A. Penirschke, C. Damm, P. Scheele, M. Wittek, C. Weil, and R. Jakoby, “Broad-band microwave characterization of liquid crystals using a temperature controlled coaxial transmission line,” IEEE Trans. Microwave Theory Tech. 53, 1937–1945 (2005).
17. S. Gauza, H. Wang, C.-H. Wen, S.-T. Wu, A. J. Seed, and R. Dambrowski, “High birefringence isothiocyanato tolane liquid crystals,” Jpn. J. Appl. Phys. 42, 3463–3466 (2003).
18. L. F. Chen, C. K. Ong, C. P. Neo, V. V. Varadan, and V. K. Varadan, Microwave Electronics (Wiley, 2004).
19. M. Tonouchi, “Cutting-edge terahertz technology,” Nat. Photon. 1, 97–105 (2007).
20. J. A. Zeitler, P. F. Taday, D. A. Newnham, M. Pepper, K. C. Gordon, and T. Rades, “Terahertz pulsed spectroscopy and imaging in the pharmaceutical setting—a review,” J. Pharm. Pharmacol. 59, 209–223 (2007).
21. E. P. J. Parrott, J. A. Zeitler, T. Friščic´, M. Pepper,W. Jones, G. M. Day, and L. F. Gladden, “Testing the sensitivity of terahertz spectroscopy to changes in molecular and supramolecular structure. a study of structurally similar cocrystals,” Cryst. Growth Design 9, 1452–1460 (2009).
22. I. Pupeza, R. Wilk, and M. Koch, “Highly accurate optical material parameter determination with THz time-domain spectroscopy,” Opt. Express 15, 4335–4350 (2007).
23. S.-T. Wu, U. Efron, and L. D. Hess, “Birefringence measurements of liquid crystals,” Appl. Opt. 23, 3911–3915 (1984).
24. R.-P. Pan, C.-F. Hsieh, C.-L. Pan, and C.-Y. Chen, “Temperature-dependent optical constants and birefringence of nematic liquid crystal 5CB in the terahertz frequency range,” J. Appl. Phys. 103, 093523 (2008).
25. K. C. Lim, J. D. Margerum, A. M. Lackner, L. J. Miller, E. Sherman, and W. H. J. Smith, “Liquid crystal birefringence for millimeter wave radar,” Liq. Cryst. 14, 327–337 (1993).
26. S. A. Jewell, E. Hendry, T. H. Isaac, and J. R. Sambles, “Tuneable Fabry-Perot etalon for terahertz radiation,” New J. Phys. 10, 033012 (2008).
27. S.-T. Wu, “Absorption measurements of liquid crystals in the ultraviolet, visible, and infrared,” J. Appl. Phys. 84, 4462–4465 (1998).